Does the Electronic Structure of Möbius Annulenes Follow Heilbronner's Ideas?

Peter B. Karadakov,*[a] David L. Cooper*[b]

Abstract: It is shown, on the example of the monocyclic cyclononatetraenyl cation, $C_9H_9^+$, that the fully-variational optimization of modern *ab initio* wavefunctions based on spin-coupled generalized valence bond (SCGVB) theory vindicates, in a surprising level of detail, essential features of Heilbronner's ideas for the electronic structure of Möbius annulenes such as the arrangement of overlapping carbon 2p atomic orbitals along a Möbius strip, leading to a phase inversion between the first and last orbitals. In the SCGVB description, the aromaticity of this Möbius system with eight π electrons follows from the extensive resonance between VB structures.

Möbius annulenes are the brainchild of Edgar Heilbronner who in 1964[1] decided to find out what would happen if the cylindrical arrangement of overlapping 2p atomic orbitals (AOs) in a conventional (Hückel) annulene, $(CH)_n$, were to be replaced by an alternative arrangement along a Möbius strip (see Figure 1). In order to obtain Hückel molecular orbital (HMO) descriptions of Möbius annulenes, Heilbronner assumed that the resonance integral $\beta_{\mu\nu}$ between a pair of 2p AOs twisted by angle $\omega_{\mu\nu}$ is related to the standard resonance integral β between a pair of parallel 2p AOs through a simple formula involving the cosine of the twist angle: $\beta_{\mu\nu} = \beta \cos \omega_{\mu\nu}$.[1] The twist angles between pairs of consecutive AOs in Heilbronner's model of a Möbius annulene with n CH units remain constant, $\omega_{\mu,\mu+1} = \pi/n$, except for $\omega_{n,1} = \pi - \pi/n$. As a result, apart from the trivial switch to "weaker" $\beta' = \beta \cos(\pi/n)$ resonance integrals, the HMO secular determinant for a Möbius annulene differs from that for its Hückel counterpart only in the signs of the resonance integrals linking centers 1 and n (see Figure 2). Analytic orbital energy expressions are just as easy to obtain as for Hückel annulenes and, in fact, this can be done even for Möbius annulenes with bond alternation.[2] According to the energy expressions shown in Figure 2, Hückel annulenes are aromatic for $n = 4\nu + 2$ and antiaromatic for $n = 4\nu$; this well-known Hückel $4\nu + 2/4\nu$ aromaticity rule is reversed for Möbius annulenes in that the aromatic cycles become those with 4ν CH units, while those with $4\nu + 2$ CH units are

Place Figure 1 near here.

Place Figure 2 near here.

[a] Dr. P. B. Karadakov
   Department of Chemistry, University of York, Heslington, York YO10 5DD (UK)
   E-mail: peter.karadakov@york.ac.uk
[b] Dr. D. L. Cooper
   Department of Chemistry, University of Liverpool, Liverpool L69 7ZD (UK)
   E-mail: dlc@liverpool.ac.uk

antiaromatic. This is particularly well-illustrated by Zimmerman's adaptation[3–5] of the familiar Frost-Musulin diagrams[6] to Möbius annulenes. In general, Hückel and Möbius orbital arrays exhibit even and odd numbers of phase changes (sign inversions), respectively;[5] the examples in Figure 1 involve no (zero) phase changes in (a) and a single phase change in (b).

Since its inception, the concept of Möbius annulenes has continued to receive considerable attention from both theoretical and experimental chemists. On the synthetic side, a Möbius aromatic hydrocarbon was first reported by Herges and co-workers in 2003;[7] a comprehensive survey of pre-2005 research on Möbius aromaticity and delocalization can be found in Rzepa's review;[8] a very recent study shows that Möbius orbital topology can be established even in acyclic systems such as linear cumulenes.[9] We would also like to draw attention to a detailed analysis carried out by McKee *et al.*[10] of the simplifications in Heilbronner's HMO treatment.

The aim of this communication is to investigate whether Heilbronner's rather simplistic but conceptually very powerful HMO-based ideas about the electronic structure of Möbius annulenes can be confirmed using advanced *ab initio* quantum-chemical methods such as the spin-coupled generalized valence bond (SCGVB) approach* and complete-active-space self-consistent field (CASSCF) theory.

The SCGVB approach is a modern form of VB theory based on a wavefunction which usually turns out to be a close approximation to its CASSCF counterpart, but can be interpreted in terms of a small number of meaningful VB resonance structures (for a review of the theory and its applications, see reference 13). One example that can now be found in several physical and organic chemistry textbooks is provided by the SCGVB description of benzene[14–16] (the Hückel 6-annulene), which is very different from the delocalized orbital model obtained using conventional MO theory. The six π electrons populate a single product of six non-orthogonal active (or, spin-coupled) orbitals, the spins of which are coupled in all five possible ways leading to an overall singlet. The optimal SC orbitals turn out to be well-localized, similar in shape to carbon 2p AOs but with small symmetrical protrusions towards neighboring carbons; the optimal spin-coupling pattern, if expressed in terms of Rumer spin functions,[17] is dominated by two equivalent Kekulé structures and has much smaller contributions from three equivalent Dewar (or para-bonded) structures. This SCGVB picture, which features a sequence of overlapping singly-occupied carbon 2p AO-like orbitals similar to that in Figure 1(a), reproduces the essential features of the well-known classical VB description of benzene in terms of resonance structures and arises directly from a good-quality wavefunction which accounts for close to 90% of the "non-dynamic" correlation energy

---

*This approach, as introduced by Gerratt,[11] has mostly been termed spin-coupled (SC or even SCVB), with an acknowledgment that the construction is equivalent to that of full generalized valence bond (full-GVB), as introduced by Goddard,[12] or it has been called (full-)GVB, with a mention of the equivalence to SC (or SCVB). It seems to the present authors to be undesirable to persist with different names for essentially identical calculations. Accordingly, we use here instead the compound term spin-coupled generalized valence bond (SCGVB) that aims to encompass both sets of names.

incorporated in a "6 in 6" π-space CASSCF wavefunction.[16]

In its original form,[11,18] as it was applied to benzene, the SCGVB wavefunction makes use of a "N in N" active space, described by means of a single product of N non-orthogonal active orbitals, multiplied by a general N-electron spin function. The "N in M" active spaces with different numbers of active electrons and active orbitals which are encountered in many CASSCF applications can be handled through an extension of SCGVB theory to "N in M" ($N \neq M$) active spaces.[19] The SCGVB(N, M) wavefunction retains the essential features of the original SCGVB model: It involves just the products of non-orthogonal orbitals corresponding to all distributions of N electrons amongst M orbitals in which the smallest number of orbitals possible, $|N - M|$, are doubly-occupied (for $N > M$) or omitted (for $N < M$), and all other active orbitals are singly-occupied; each of these products is combined with a flexible spin function which allows any mode of coupling of the spins of the active orbitals within the product.

The ring system we have chosen for this study is the monocyclic cyclononatetraenyl cation, $C_9H_9^+$, which was shown by Mauksch *et al.*[20] to be Möbius-aromatic at its lowest-energy C_2 geometry. In Heilbronner's model, the $C_9H_9^+$ ring includes eight π electrons and nine carbon 2p AOs, which suggests a "8 in 9" active space. Accordingly, we describe here the electronic structure of the cyclononatetraenyl cation by means of SCGVB(8,9) and CASSCF(8,9) wavefunctions.

The C_2 geometry of the $1\,^1$A electronic ground state of $C_9H_9^+$ was optimized at the MP2/aug-cc-pVDZ level of theory with GAUSSIAN16[21] using the default frozen-core ("FC") approximation, under the "VeryTight" convergence criteria. The optimized geometry was verified as a local minimum through diagonalization of the MP2/aug-cc-pVDZ analytic nuclear Hessian. The lowest harmonic frequency, corresponding to a normal mode of B symmetry, was obtained as 179.6 cm^{-1}. The differences from the B3LYP/6-311+G(d,p) geometry reported by Mauksch *et al.*[20] are relatively minor: As shown in Figure 3, MP2/aug-cc-pVDZ yields slightly longer carbon-carbon bond lengths. Fully-variational SCGVB(8,9) and CASSCF(8,9) calculations were carried out for the $1\,^1$A electronic ground state at the MP2/aug-cc-pVDZ optimized geometry, using the aug-cc-pVDZ and aug-cc-pVTZ basis sets. For the SCGVB(8,9) calculations we used the CASVB algorithms[22–25] implemented in MOLPRO.[26,27] The CASSCF(8,9) calculations were performed both with GAUSSIAN16[21] and with MOLPRO,[26,27] which produced identical results; additionally, the nine active space orbitals from the CASSCF(8,9) calculations were localized using the Foster-Boys procedure[28] implemented in GAUSSIAN16. Given that the results obtained with the aug-cc-pVDZ and aug-cc-pVTZ basis sets were found to be very similar, we can be confident that our model for the electronic structure of $C_9H_9^+$ will remain essentially the same within even larger basis sets and that none of its features can be attributed to any sort of basis set incompleteness. We report here only the results obtained with the aug-cc-pVDZ basis set;

Place Figure 3 near here.

our experience with SCGVB and CASSCF calculations suggests that all essential features of the orbital models for $C_9H_9^+$ discussed in this communication could also be reproduced with smaller basis sets, such as cc-pVDZ or even 6-31G. As can be seen in Table 1, the SCGVB(8,9) wavefunction manages to account for a surprisingly large proportion of the non-dynamic correlation energy achievable in an "8 in 9" active space, even though it uses a much smaller number of configuration state functions (CSFs) than the CASSCF(8,9) construction. Of course, the MP2 energy, which includes dynamic correlation effects for all electrons, is significantly lower.

The shapes of the nine non-orthogonal SC orbitals from the SCGVB(8,9) wavefunction are superimposed in Figure 3(a). Despite the twisted structure of $C_9H_9^+$, all of these orbitals are very similar in appearance. Clearly, they closely resemble the distorted carbon 2p AOs with small symmetrical protrusions towards neighboring carbons that are familiar from the SCGVB description of benzene.[14–16] It is important to emphasize that the SCGVB(8,9) wavefunction for the monocyclic cyclononatetraenyl cation was optimized without any symmetry or other constraints which could have influenced the shapes of the SC orbitals. Comparison of Figure 3(a) to Figure 1(b) shows that the SC orbitals for $C_9H_9^+$ closely reproduce the sequence of twisted carbon 2p AOs arranged along a Möbius strip; in this way, the SCGVB(8,9) model of $C_9H_9^+$ provides a convincing vindication of Heilbronner's ideas about the electronic structure of Möbius annulenes. It should be mentioned that the SC orbitals $\psi_1-\psi_9$ need not emerge from the SCGVB(8,9) calculation with their phases aligned as shown in Figure 3(a). Instead, each of these orbitals is determined up to an arbitrary sign factor so that changing the sign factor of one orbital introduces two phase changes between that orbital and its two neighboring orbitals, retaining the overall parity of the phase changes within the orbital array. The position of the phase change within the orbital array is arbitrary, just as in Heilbronner's model, where it depends on the choice of the first and last orbitals in the numbering scheme. With the choice of orbital phases shown in Figure 3(a), the SC orbitals transform under the $\hat{C}_2$ rotation as $\hat{C}_2\psi_1 = -\psi_9$, $\hat{C}_2\psi_2 = \psi_8$, $\hat{C}_2\psi_3 = \psi_7$, $\hat{C}_2\psi_4 = \psi_6$ and $\hat{C}_2\psi_5 = -\psi_5$.

The close correspondence between Heilbronner's ideas and the SCGVB(8,9) description of the monocyclic cyclononatetraenyl cation is confirmed by the overlap integrals between the SC orbitals from Figure 3(a). As can be seen from Table 2, the overlap integrals between consecutive SC orbitals around the ring, $\langle\psi_\mu|\psi_{\mu+1}\rangle$, are all positive with the exception of $\langle\psi_1|\psi_9\rangle$, which is negative as a result of the phase inversion. Due to the small size of the $C_9H_9^+$ ring and its twisted structure, some overlap integrals between non-neighboring SC orbitals also have relatively large magnitudes, such as $\langle\psi_1|\psi_3\rangle = \langle\psi_7|\psi_9\rangle = -0.429$. The 16 most important VB structures (non-orthogonal CSFs) included in the SCGVB(8,9) wavefunction for $C_9H_9^+$ are shown in Figure 4. These 16 VB structures occur as 8 symmetry-related pairs, connected through the $\hat{C}_2$ rotation. For example, the first VB structure and its

4

symmetry partner (not shown in Figure 4) can be written down (in unnormalized form) as

$$\hat{C}_2 \hat{A}\left[(54)\psi_2\psi_3\psi_4\psi_5\psi_7\psi_8\psi_9\psi_1(\alpha\beta-\beta\alpha)(\alpha\beta-\beta\alpha)(\alpha\beta-\beta\alpha)(\alpha\beta-\beta\alpha)\right]$$
$$= \hat{A}\left[(54)\psi_2\psi_3\psi_5\psi_6\psi_7\psi_8\psi_9\psi_1(\alpha\beta-\beta\alpha)(\alpha\beta-\beta\alpha)(\alpha\beta-\beta\alpha)(\alpha\beta-\beta\alpha)\right]$$

where "(54)" stands for the 54 core electrons, accommodated in 27 doubly-occupied optimized orbitals. We report both Chirgwin-Coulson weights,[29] which are the most usual choice in applications of VB theory, and also inverse-overlap Gallup-Norbeck weights,[30] which have the advantage of always being non-negative. Despite the fact that the individual weights of the 16 VB structures are relatively low (none of these exceeds 6%), the sums of these weights are *ca.* 55% and *ca.* 60% for the Chirgwin-Coulson and Gallup-Norbeck weights, respectively. This is an indication that these 16 VB structures account for the majority of the SCGVB(8,9) wavefunction. (Any other VB structure has a Chirgwin-Coulson weight under 2%.) Each of the 16 VB structures shown in Figure 4 involves singlet couplings of three pairs of SC orbitals involved in shorter carbon-carbon bonds, (ψ_1, ψ_2), (ψ_2, ψ_3), (ψ_4, ψ_5), (ψ_5, ψ_6), (ψ_7, ψ_8) and (ψ_8, ψ_9). This situation is reminiscent of the resonance between Kekulé and Dewar (or para-bonded) structures in benzene and strongly suggests that the electronic ground state of the monocyclic cyclononatetraenyl cation is aromatic. Just two of these 16 VB structures involve singlet coupling of SC orbitals ψ_1 and ψ_9; this is an indication that the most appropriate choice for the phase change location is between those two orbitals, as shown in Figure 3(a).

Foster-Boys localization of the active space orbitals from the CASSCF(8,9) wavefunction for $C_9H_9^+$ produces a set of localized orbitals which, when phase-aligned in a similar fashion to the SC orbitals (*vide supra*), look very similar to the set of SC orbitals for this system, as demonstrated by Figures 3(a) and (b). While this can be viewed as an alternative and perhaps more straightforward way of verifying Heilbronner's ideas, the SCGVB picture offers important additional insights. An examination of more detailed pictures of the two types of orbital, such as those for ψ_5, shown as $\psi_5 = \pm 0.03$ isosurfaces in Figure 3(c), and the corresponding localized CASSCF(8,9) active-space orbital, shown in Figure 3(d), reveals that the non-orthogonal SC orbitals spread out more over adjacent atomic centers. This allows the establishment of the meaningful orbital overlap pattern reported in Table 2, whereas the more compact localized CASSCF(8,9) orbital needs to have inversed-phase "tails" on adjacent atomic centers so as to ensure its orthogonality to neighboring localized orbitals. Furthermore, the localization of the active space orbitals from the CASSCF(8,9) wavefunction for $C_9H_9^+$ does not provide any help with the analysis of the physical relevance of the thousands of CSFs included in this wavefunction.

We have demonstrated in this communication, on the example of the monocyclic cyclononatetraenyl cation, $C_9H_9^+$, how the fully-variational optimization of modern *ab initio* wavefunctions based on SCGVB theory vindicates, in a surprising level of detail, essential features of Heilbronner's ideas[1] for the electronic structure of Möbius annulenes.

Conflict of interest

The authors declare no conflict of interest.

[1] E. Heilbronner, *Tetrahedron Lett.* **1964**, *29*, 1923–1928.

[2] P. Karadakov, V. Enchev, F. Fratev, O. Castaño, *Chem. Phys. Lett.* **1981**, *83*, 529–532.

[3] H. E. Zimmerman, *J. Am. Chem. Soc.* **1966**, *88*, 1564–1565.

[4] H. E. Zimmerman, *J. Am. Chem. Soc.* **1966**, *88*, 1566–1567.

[5] H. E. Zimmerman, *Acc. Chem. Res.* **1971**, *4*, 272–280.

[6] A. A. Frost AA, B. Musulin, *J. Chem. Phys.* **1953**, *21*, 572–573.

[7] D. Ajami, O. Oeckler, A. Simon, R. Herges, *Nature* **2003**, *426*, 819–821.

[8] H. S. Rzepa, *Chem. Rev.* **2005**, *105*, 3697–3715.

[9] M. H. Garner, R. Hoffmann, S.Rettrup, G. C. Solomon, *ACS Cent. Sci.* **2018**, *4*, 688–700.

[10] W. C. McKee, J. I. Wu, H. S. Rzepa, P. v. R. Schleyer, *Org. Lett.* **2013**, *15*, 3432–3435.

[11] J. Gerratt, W. N. Lipscomb, *Proc. Natl. Acad. Sci. U. S. A.* **1968**, *59*, 332–335.

[12] R. C. Ladner, W. A. Goddard III, *J. Chem. Phys.* **1969**, *51*, 1073–1087.

[13] D. L. Cooper, P. B. Karadakov, *Int. Rev. Phys. Chem.* **2009**, *28*, 169–206.

[14] D. L. Cooper, J. Gerratt, M. Raimondi, *Nature* **1986**, *323*, 699–701.

[15] J. Gerratt, *Chem. Br.* **1987**, *23*, 327–329.

[16] D. L. Cooper, S. C. Wright, J. Gerratt, P. A. Hyams, M. Raimondi, *J. Chem. Soc. Perkin Trans. II* **1989**, 719–724.

[17] G. Rumer, *Göttinger Nachr.* **1932**, *3*, 337–341.

[18] P. B. Karadakov, J. Gerratt, D. L. Cooper, M. Raimondi, *J. Chem. Phys.* **1992**, *97*, 7637–7655.

[19] P. B. Karadakov, D. L. Cooper, B. J. Duke, J. Li, *J. Phys. Chem. A* **2012**, *116*, 7238–7244.

[20] M. Mauksch, V. Gogonea, H. Jiao, P. v. R. Schleyer, *Angew. Chem. Int. Ed.* **1998**, *37*, 2395–2397; *Angew. Chem.* **1998**, *110*, 2515–2517.

[21] M. J. Frisch, G. W. Trucks, H. B. Schlegel, G. E. Scuseria, M. A. Robb, J. R. Cheeseman, G. Scalmani, V. Barone, G. A. Petersson, H. Nakatsuji, X. Li, M. Caricato, A. V. Marenich, J. Bloino, B. G. Janesko, R. Gomperts, B. Mennucci, H. P. Hratchian, J. V. Ortiz, A. F. Izmaylov, J. L. Sonnenberg, D. Williams-Young, F. Ding, F. Lipparini, F. Egidi, J. Goings, B. Peng, A. Petrone, T. Henderson, D. Ranasinghe, V. G. Zakrzewski, J. Gao, N. Rega, G. Zheng, W. Liang, M. Hada, M. Ehara, K. Toyota, R. Fukuda, J. Hasegawa, M. Ishida, T. Nakajima, Y. Honda, O. Kitao, H. Nakai, T. Vreven, K. Throssell, J. A. Montgomery, Jr., J. E. Peralta, F. Ogliaro, M. J. Bearpark, J. J. Heyd, E. N. Brothers, K. N. Kudin, V. N. Staroverov, T. A. Keith, R. Kobayashi, J. Normand, K. Raghavachari, A. P. Rendell, J. C. Burant, S. S. Iyengar, J. Tomasi, M. Cossi, J. M. Millam, M. Klene, C. Adamo, R. Cammi, J. W. Ochterski, R. L. Martin, K. Morokuma, O. Farkas, J. B. Foresman, and D. J. Fox, *Gaussian 16, Revision A.03*, Gaussian, Inc., Wallingford CT, **2016**, www.gaussian.com.

[22] T. Thorsteinsson, D. L. Cooper, J. Gerratt, P. B. Karadakov, M. Raimondi, *Theor. Chim. Acta*, **1996**, *93*, 343–366.

[23] D. L. Cooper, T. Thorsteinsson, J. Gerratt, *Adv. Quant. Chem.* **1998**, *32*, 51–67.

[24] T. Thorsteinsson, D. L. Cooper, *J. Math. Chem.* **1998**, *23*, 105–126.

[25] T. Thorsteinsson, D. L. Cooper, in *Quantum Systems in Chemistry and Physics. Volume 1: Basic Problems and Model Systems* (Eds. A. Hernández-Laguna, J. Maruani, R. McWeeny, S. Wilson), Kluwer, Dordrecht, **2000**, pp. 303–326.

[26] H.-J. Werner, P. J. Knowles, G. Knizia, F. R. Manby, M. Schütz, *WIREs Comput. Mol. Sci.* **2012**, *2*, 242–253.

[27] H.-J. Werner, P. J. Knowles, G. Knizia, F. R. Manby, M. Schütz, P. Celani, W. Györffy, D. Kats, T. Korona, R. Lindh, A. Mitrushenkov, Rauhut, G.; Shamasundar, K. R.; Adler, T. B.; Amos, R. D.; Bernhardsson, A.; Berning, A.; D. L.Cooper, M. J. O. Deegan, A. J. Dobbyn, F. Eckert, E. Goll, C. Hampel, A. Hesselmann, G. Hetzer, T. Hrenar, G. Jansen, C. Köppl, Y. Liu, A. W. Lloyd, R. A. Mata, A. J. May, S. J. McNicholas, W. Meyer, M. E. Mura, A. Nicklass, D. P. O'Neill, P. Palmieri, D. Peng, K. Pflüger, R. Pitzer, M. Reiher, T. Shiozaki, H. Stoll, A. J. Stone, R. Tarroni, T. Thorsteinsson, M. Wang, *MOLPRO, Version 2015.1, A Package of Ab Initio Programs*, Cardiff, **2015**, www.molpro.net.

[28] J. M. Foster, S. F. Boys, *Rev. Mod. Phys.* **1960**, *32*, 300–302.

[29] B. H. Chirgwin, C. A. Coulson, *Proc. Roy. Soc. Lond. Ser. A* **1950**, *201*, 196–209.

[30] G. A. Gallup, J. M. Norbeck, *Chem. Phys. Lett.* **1973**, *21*, 495–500.

Tables and Figures

Table 1. Total HF, SCGVB(8,9), CASSCF(8,9) and MP2 energies (in E_h) of the $1\,^1A$ electronic ground state of $C_9H_9^+$, percentages of recovered CASSCF(8,9) correlation energy (in brackets), and numbers of CSFs included in the SCGVB(8,9) and CASSCF(8,9) wavefunctions (aug-cc-pVDZ basis, MP2/aug-cc-pVDZ geometry, frozen-core MP2).

Wavefunction	CSFs	Total Energy	
HF	1	$-345.727\,326$	(0.0%)
SCGVB(8,9)	126^a	$-345.833\,582$	(93.4%)
CASSCF(8,9)	5292^a	$-345.841\,151$	(100.0%)
MP2		$-346.957\,966$	

^{a} Without taking symmetry into account. There are 64 symmetry-unique non-orthogonal CSFs (VB structures) and 2676 A symmetry CSFs in the $1\,^1A$ SCGVB(8,9) and CASSCF(8,9) wavefunctions, respectively.

Table 2. Overlap integrals $\langle\psi_\mu|\psi_\nu\rangle$ between the SC orbitals from the SCGVB(8,9)/aug-cc-pVDZ wavefunction for $C_9H_9^+$. Positive and negative overlap integrals between neighboring SC orbitals highlighted in blue and red, respectively.

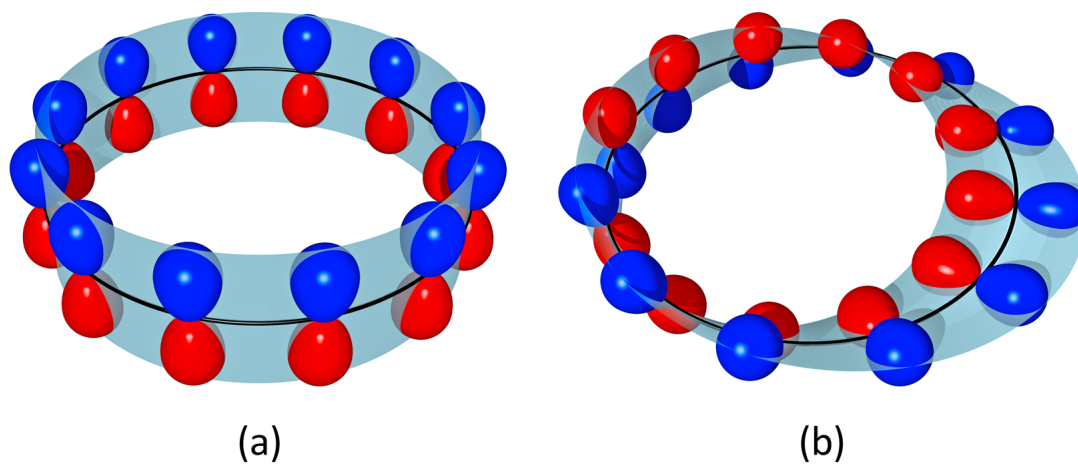|	ψ_1	ψ_2	ψ_3	ψ_4	ψ_5	ψ_6	ψ_7	ψ_8	ψ_9
ψ_1	1.000	0.332	−0.429	−0.338	0.066	0.300	0.300	0.044	−0.495
ψ_2		1.000	0.413	−0.202	−0.085	0.074	−0.006	0.029	0.044
ψ_3			1.000	0.419	−0.077	−0.233	−0.186	−0.006	0.300
ψ_4				1.000	0.404	−0.331	−0.233	0.074	0.300
ψ_5					1.000	0.404	−0.077	−0.085	0.066
ψ_6						1.000	0.419	−0.202	−0.338
ψ_7							1.000	0.413	−0.429
ψ_8								1.000	0.332
ψ_9									1.000

Figure 1. Conventional (Hückel) 12-annulene (a) and Möbius 12-annulene (b). Note the phase change between the two leftmost 2p orbitals in (b).

$$\begin{vmatrix} \alpha-\epsilon & \beta & & & \beta \\ \beta & \alpha-\epsilon & \beta & & \\ & \beta & \ddots & \ddots & \\ & & \ddots & \ddots & \beta \\ \beta & & & \beta & \alpha-\epsilon \end{vmatrix} \qquad \begin{vmatrix} \alpha-\epsilon & \beta' & & & -\beta' \\ \beta' & \alpha-\epsilon & \beta' & & \\ & \beta' & \ddots & \ddots & \\ & & \ddots & \ddots & \beta' \\ -\beta' & & & \beta' & \alpha-\epsilon \end{vmatrix}$$

$$\underbrace{}_{\text{Hückel } n\text{-annulene}} \qquad \underbrace{}_{\text{Möbius } n\text{-annulene}}$$

$$\epsilon_k = \alpha + 2\beta\cos\frac{2\pi k}{n} \qquad\qquad \epsilon_k = \alpha + 2\beta'\cos\frac{\pi(2k+1)}{n}$$

$$k = 0, 1, 2, \ldots, n-1$$

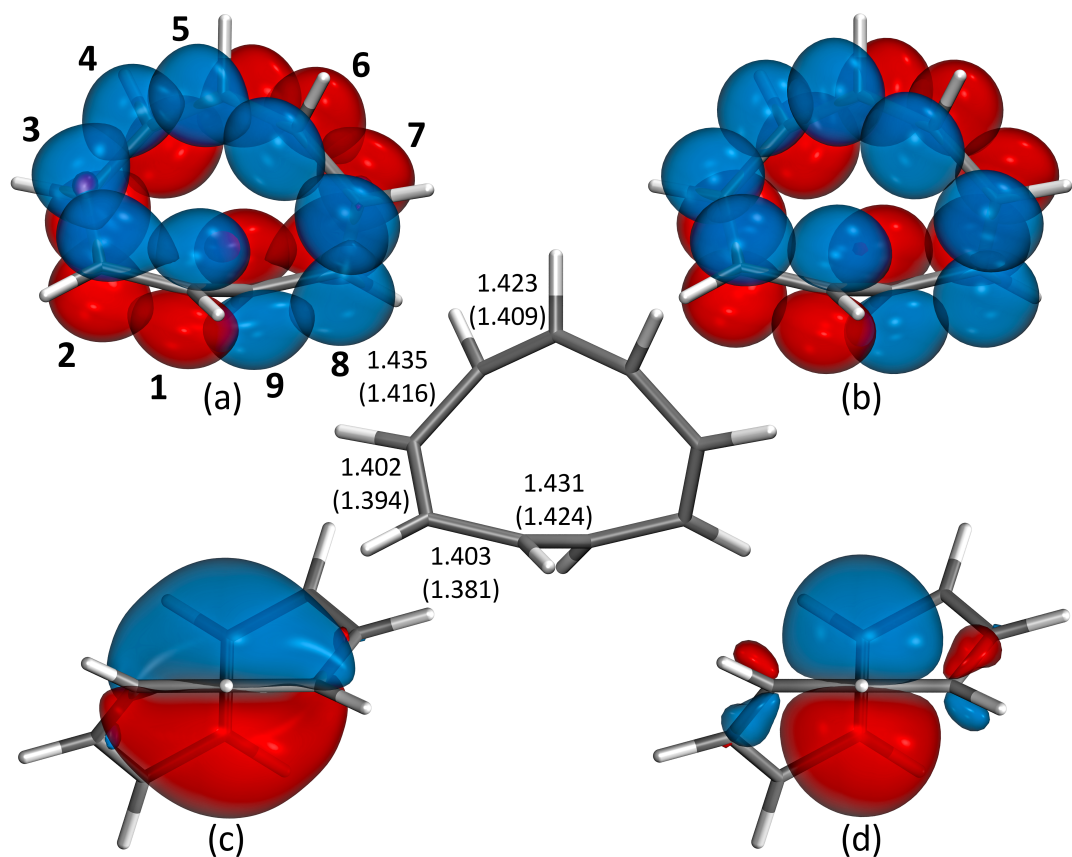**Figure 2.** HMO secular determinants and orbital energy expressions for Hückel and Möbius n-annulenes.

Figure 3. Center: MP2/aug-cc-pVTZ optimized C_2 geometry of the $1\,^1\text{A}$ electronic ground state of $C_9H_9^+$ with carbon-carbon bond lengths, B3LYP/6-311+G(d,p) bond lengths[20] in brackets, all in Å. SC orbitals $\psi_1-\psi_9$ from the SCGVB(8,9)/aug-cc-pVTZ wavefunction (a) and Foster-Boys localized active space orbitals from the CASSCF(8,9)/aug-cc-pVTZ wavefunction (b) as isovalue surfaces at $\psi_\mu = \pm0.1$. SC orbital ψ_5 (c) and corresponding Foster-Boys localized active space orbital (d) as isovalue surfaces at $\psi_\mu = \pm0.03$.

2×5.531 (2×3.862)　　2×4.665 (2×2.818)　　2×4.042 (2×5.846)　　2×2.954 (2×3.518)

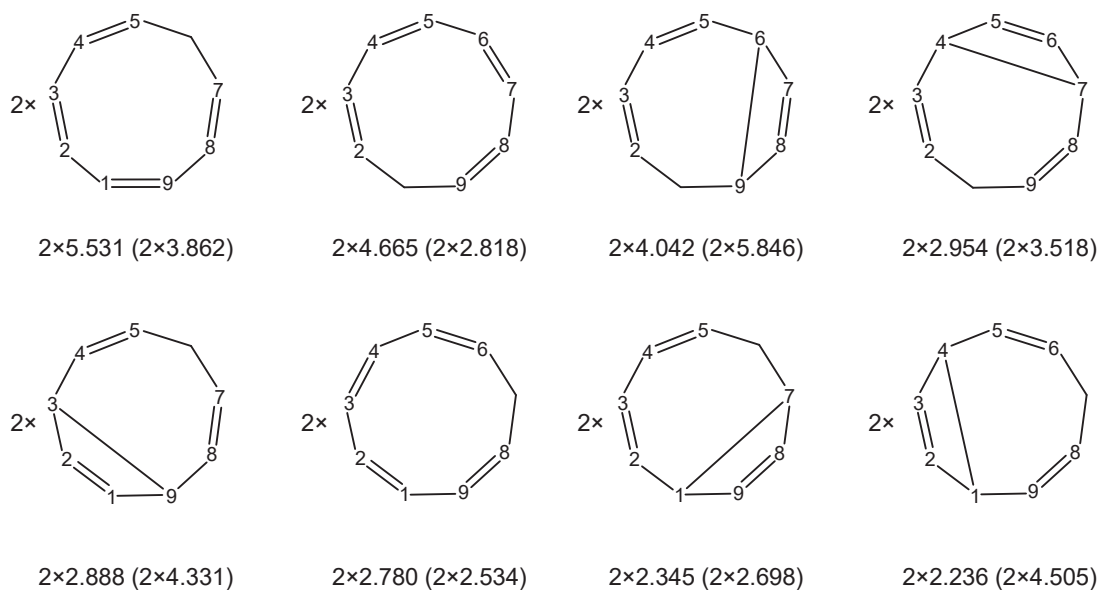2×2.888 (2×4.331)　　2×2.780 (2×2.534)　　2×2.345 (2×2.698)　　2×2.236 (2×4.505)

Figure 4. 16 VB structures with highest weights included in the SCGVB(8,9) wavefunction for $C_9H_9^+$, shown as 8 symmetry-related pairs. The numbers correspond to the numbering of the SC orbitals in Figure 3(a); a double line denotes singlet pairing of the spins of the respective orbitals. Chirgwin-Coulson weights and Gallup-Norbeck weights (in brackets) in %. For further details, see text.

Entry for the Table of Contents

Peter B. Karadakov,* David L. Cooper*

Does the Electronic Structure of Möbius Annulenes Follow Heilbronner's Ideas?
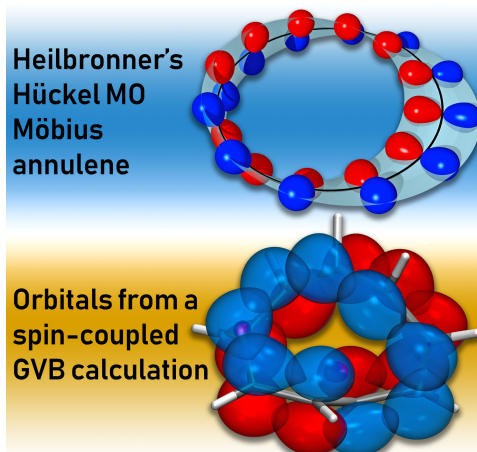
Was Heilbronner right? In 1964 Heilbronner came up with the idea of a congugated cycle twisted in a Möbius ring and described it using simple Hückel molecular orbitals. Advanced spin-coupled generalized valence bond (SCGVB) calculations on $C_9H_9^+$ provide a surprisingly clear vindication of this intuitive and very useful concept, showing a set of overlapping single-electron orbitals with a single negative overlap (see picture).